Appendix C

Specifications and transformations for the Vanderbilt experiment.

This appendix consists on tables with the numerical results of the transformations of the Vanderbilt database. The first tables summarises the physical specifications of the images. The second table shows the values of the transformations obtained with our method, with two setting: rigid (R), i.e., 3 translation plus 3 rotations parameters, and including scaling (S), which has 3 extra scale parameters..

The third table gives the initial alignment translations. For some patients the values are very high in the z–axis, thus indicating the necessity of this alignment. Corresponding translation values of the transformation table are mostly low, which indicates that the initial guess if fairly close to the final value.

Patient	Pixel size (mm)	Slice thickness (mm)	Pixels	Slices	Modality
1–7 A	0.65	4	512	28-43	CT
	1.25	4	256	20-26	T1
	1.25	4	256	20-26	T2
	1.25	4	256	20-26	PD
1–9 B	0.4 - 0.45	3	512	40-49	CT
	0.78 - 0.86	3	256	51-52	T1
	0.78 - 0.86	3	256	52	T2
	0.78 - 0.86	3	256	52	PD
	1	1.25-1.66	256	128	RAGE

Table C.1: Image specifications of the Vandebilt's database

Modality	Translation (pixels)			Rotation (deg)			Scaling			Correlation	Method
	x	y	z	x	y	z	x	y	z		
Patient 1–A											
ct–	0.2	0.1	2.7	2.8	-1.2	0.5				1313	R
mr_PD	-0.5	-3.8	-3.6	2.8	-0.6	0.7	0.993	0.976	0.946	1568	S
ct–	0.6	2.3	0.1	-1.5	0	0.5				1557	R
mr_PDR	1.3	1.9	0.1	-1.5	0	0.5	1.003	0.998	0.997	1569	S
ct–	1	2.7	-2.3	-1.8	0	0				1562	R
mr_T1	1	2.4	-2.9	-0.9	0	0	1	0.999	0.991	1575	S
ct–	1	1.8	-2.1	0.7	0	0.8				1688	R
mr_T1R	1.2	2.8	-0.4	0	-0.8	0.2	1.003	1.003	1.019	1723	S
ct–	1.6	3.5	-8.2	-2	-1.9	1				1317	R
mr_T2	2.9	-0.8	-11	-1.3	-1.6	0.7	1.006	0.977	0.976	1424	S
ct–	2.1	2.8	-3.8	1.7	-0.1	0.1				1270	R
mr_T2R	5.1	3	-3.9	0.8	-0.1	0.7	1.016	0.998	0.988	1359	S
Patient 2–A											
ct–	-5	17.4	1.5	1.4	0	0				1540	R
mr_PD	-5.8	17.2	-2.6	0.9	-0.2	0	0.996	0.998	0.957	1613	S
ct–	-4.9	15.5	1.5	-1.6	0	0				1828	R
mr_PDR	-4.8	14.4	-1.2	-1.4	0	0	1	0.995	0.968	1940	S
ct–	-2.9	17.3	-4	-2.1	0	0				1366	R
mr_T1	-2.8	18.6	-6.5	-2	0	0	1	1.007	0.968	1432	S
ct–	-2.9	14.9	-3.2	0	-0.3	0				1550	R
mr_T1R	-2.9	15	-3	0	0	0	1	1	0.999	1578	S
ct–	-3	19.5	-7.3	1	0	0				1376	R
mr_T2	-1.8	21.2	-6.7	0.9	-0.9	0.2	1.007	1.009	0.996	1464	S
ct–	-5.1	24	-32.3	0	5	0				866	R
mr_T2R	0	27.6	-38.8	-3.3	0.2	-0.2	1.022	1.017	0.871	1155	S
Patient 3–A											
ct–	-4.3	-1.4	2.4	0.4	-0.1	-0.7				1331	R
mr_PD	-5.8	-3.3	-0.2	-0.5	0	0	0.991	0.986	0.986	1536	S
ct–	-3.9	-3	1.9	0	0	0				1375	R
mr_PDR	-4	-3.7	1.7	-0.2	-0.2	-0.1	0.999	0.993	0.998	1382	S
ct–	-0.3	-6.6	3.7	4.2	1.4	-1.4				894	R
mr_T1	-2.5	-8.5	-1.9	-1.1	-1	0.5	0.991	0.976	0.97	1097	S
ct–	-0.3	-4.7	7.6	-2.2	1.4	-0.6				938	R
mr_T1R	-3.3	-10.6	6.6	-0.7	0.7	-1.2	0.985	0.974	1.002	1058	S
ct–	-3	-0.4	-3.6	-2	0	0				1326	R
mr_T2	-2.9	-1.4	-4.4	-2.1	0	0	1	0.994	0.994	1351	S
ct–	-2.9	-1.6	-5.1	-2.5	0	0				1405	R
mr_T2R	-1.1	-1.7	-4.5	-2.4	0	-0.1	1.008	0.998	1.004	1427	S
Patient 4–A											
ct–	-3.2	11	1.5	0	-2.4	0				1157	R

Modality	Translation (pixels)			Rotation (deg)			Scaling			Correlation	Method
	x	y	z	x	y	z	x	y	z		
mr_PD	-3.9	9.1	0.7	-0.4	-1.2	0	0.994	0.988	0.999	1222	S
ct–	-1.9	8.8	2.2	-0.6	0	0				1198	R
mr_PDR	-2.7	6.6	-0.3	-1.3	0.6	0	0.996	0.986	0.979	1272	S
ct–	-0.9	9.6	4.2	5.4	-1.7	0.2				810	R
mr_T1	-4.2	8	-15.7	-2.4	1	0	0.978	0.971	0.785	946	S
ct–	-1.7	9.6	7.5	-3.8	-0.5	0				929	R
mr_T1R	-5.7	4.5	7.5	-2.7	2.2	-1.4	0.968	0.978	1.011	1095	S
ct–	-1.9	18.7	-2.5	-0.6	0	0				1251	R
mr_T2	-1.9	18.6	-2.6	-0.4	0	0	1	0.998	0.998	1263	S
ct–	-1.9	9.2	-2.8	-1.1	0	0				1507	R
mr_T2R	-0.3	10.2	-3.2	-1.6	-0.4	-0.2	1.01	1.003	0.993	1570	S
Patient 5–A											
ct–	-0.7	0.2	1.1	-3.1	0.2	-0.7				2165	R
mr_PD	-0.7	-0.7	0.7	-2.9	0.1	-0.7	1	0.995	0.996	2189	S
ct–	-0.9	-0.5	1	-3.2	0	0				2348	R
mr_PDR	-1	-2.3	1.5	-1.9	0	0	0.999	0.992	1.004	2477	S
ct–	-1.4	-1.9	1.4	-2.6	0.3	-0.5				2007	R
mr_T1	-1.5	-3.4	-2.4	-2.5	0.1	-0.5	0.999	0.992	0.963	2147	S
ct–	-2	-3.3	1.5	-2.9	0	0				2123	R
mr_T1R	-2	-5.6	1	-2.9	0	0	0.999	0.987	0.995	2271	S
ct–	-1	-1.8	-17	-4.2	0	0				1627	R
mr_T2	1.7	-0.8	-17.1	-3.7	0.1	-0.4	1.018	1.004	0.991	1847	S
ct–	-1.4	-1.5	-17	-2.7	-0.6	-0.1				1746	R
mr_T2R	1.6	-1.2	-15.2	-2.9	-0.7	-0.4	1.018	0.999	1.011	1961	S
Patient 6–A											
ct–	1.5	8.4	3.3	0.8	-0.7	-0.2				1515	R
mr_PD	0	7.2	1.3	0.1	-1.2	0	0.991	0.992	0.985	1621	S
ct–	2.5	8.2	4.1	-1.5	-0.4	0.5				1449	R
mr_PDR	3.8	4.4	-0.6	-0.5	0	0	1.008	0.981	0.955	1750	S
ct–	4.4	6	-2.6	0.1	-0.6	0				1190	R
mr_T1	6.7	9.6	-4.2	-1.3	-1.5	0.5	1.014	1.014	0.974	1365	S
ct–	3.9	8	0	0	0	0				1535	R
mr_T2	5	7.4	0.9	0	0	0	1.008	0.995	1.009	1570	S
ct–	4.1	9.6	-0.5	-1.2	-0.1	0				1394	R
mr_T2R	8.7	9.2	-1.5	-2.1	-0.4	-0.1	1.025	0.994	0.985	1710	S
Patient 7–A											
ct–	-0.4	4.7	1.2	-2.3	-1	-0.2				1488	R
mr_PD	-1.8	1.2	-0.7	-0.5	-1.5	-0.1	0.991	0.983	0.982	1756	S
ct–	0	8.9	1.5	-1.6	0	0				1544	R
mr_PDR	1.1	7.8	-0.6	-0.3	-0.8	0.2	1.005	0.995	0.97	1595	S
ct–	3	2.8	-1.5	-0.5	0	0				1322	R

Modality	Translation (pixels)			Rotation (deg)			Scaling			Correlation	Method
	x	y	z	x	y	z	x	y	z		
mr_T1	4.1	4.3	-4.3	-1.9	0	0	1.005	1.01	0.962	1345	S
ct–	2.1	1.6	-1.2	1	-0.2	0.1				1517	R
mr_T1R	4.7	2.2	-1.6	1	-1.1	0.4	1.014	1	0.989	1627	S
ct–	0.5	6	-1.7	-1.3	-0.7	-0.2				1524	R
mr_T2	1.8	4.8	-1.2	-1.1	-0.1	0	1.007	0.994	1.003	1559	S
ct–	0.9	8.7	-3.4	-0.5	0.1	0				1538	R
mr_T2R	3.6	9.1	-0.2	-1.3	0.3	0.1	1.016	0.998	1.031	1706	S
Patient 1–B											
ct–	-2	-3.5	-3	1	-8.4	-3.8				2164	R
mr_PD	-2	-6.6	-6	4.2	-7.7	-3.9	0.997	0.986	0.969	2576	S
ct–	-2.9	-3.3	-3.9	3.6	-7.8	-5.2				2204	R
mr_T1	-3.2	-4.4	-5.4	3.6	-7.6	-5.1	0.996	0.992	0.984	2391	S
ct–	-1.3	2.6	-16.4	1.9	-7.4	-3.1				1724	R
mr_T2	0	1.5	-14.5	2.3	-8.2	-3.9	1.015	0.989	1.019	1921	S
mr_MP–	-1.8	7.2	-20.2	-3.7	-2.8	0.7				1712	R
mr_T2	5.1	7.6	-25.7	-5.1	0.1	-0.4	1.041	1.001	0.931	2084	S
Patient 2–B											
ct–	-8.1	-11.1	-0.2	3.3	0	-7.6				2587	R
mr_PD	-7.8	-12.9	-3.3	4.5	0.3	-7.4	1.004	0.988	0.976	3017	S
ct–	-8.2	-10.9	0	0	0	-7.2				2067	R
mr_T1	-8.6	-13.7	-5.4	4.2	0.6	-7.3	0.998	0.984	0.962	2676	S
ct–	-9	-9.3	-2.5	4.3	0.3	-7.7				2634	R
mr_T2	-7.3	-9.6	-2.7	4.3	0.1	-7.7	1.016	0.998	0.995	2853	S
mr_MP–	0	0.6	-1.7	3.2	4.3	2.9				2027	R
mr_T2	2.9	2.3	-3.1	-0.8	-0.4	-0.2	1.03	1.006	0.985	2476	S
Patient 3–B											
ct–	-1.9	8.9	-0.6	-4.2	0	0				2013	R
mr_PD	-2	8.1	-1.8	-4.3	0	0	0.999	0.997	0.99	2048	S
ct–	0.1	2.3	1.3	-5.7	-0.1	0				1896	R
mr_T1	-1.4	-1.9	-5.1	-2.6	-0.4	-0.2	0.984	0.98	0.956	2869	S
Patient 4–B											
ct–	-5.3	0.5	0.7	-4.2	-5	0.4				2578	R
mr_PD	-4.9	-2.3	-1.7	-2.2	-5.5	0.4	1.002	0.984	0.981	2862	S
ct–	-4.1	-0.1	1.1	-4.4	-5.4	0.5				2145	R
mr_T1	-4.4	-4.1	-2.7	-1.3	-5.9	0.2	0.993	0.979	0.973	2711	S
ct–	-2.3	3	-3.6	-2.1	-6.7	0				2102	R
mr_T2	-0.6	4.5	-2.2	-3.2	-5.5	0.3	1.016	1.005	1.007	2427	S
mr_MP–	2.6	6.2	-3.6	2.3	-7.5	-7				1241	R
mr_T2	5.9	6.6	-7	0.7	-0.9	-2.6	1.04	0.997	0.982	1497	S
Patient 5–B											
ct–	0.9	-4.8	3.9	11.6	2.3	-5.4				1699	R

Modality	Translation (pixels)			Rotation (deg)			Scaling			Correlation	Method
	x	y	z	x	y	z	x	y	z		
mr_T1	-0.7	-4.8	1.3	11.6	0.6	-4.7	0.983	1	0.98	1809	S
ct–	1	-7.1	-3.6	16.2	-0.8	-4.4				1976	R
mr_T2	2.4	-7.6	-0.9	16	-0.3	-4.7	1.014	0.997	1.021	2134	S
mr_MP–	1.1	1.1	-1.2	-13.8	13.3	4.5				1810	R
mr_T2	4.5	-1.2	-1	-12.6	12.4	4.9	1.029	0.977	1	1958	S
Patient 6–B											
ct–	2.1	1.1	-5.9	7.6	-2.7	-1.6				2048	R
mr_T1	3.4	0.1	-10.9	8.6	-1.9	-1.3	1.009	0.99	0.96	2245	S
ct–	1.9	4.8	-6.7	5.8	-2	-1.9				2162	R
mr_T2	2.5	2.5	-7.8	7.9	-2	-1.4	1.004	0.986	0.994	2217	S
mr_MP–	1.1	2.8	-4.8	-2.4	-6.5	1.4				2056	R
mr_T2	3.2	2.6	-3.4	-3.2	-3.6	3.3	1.023	0.995	1.003	2276	S
Patient 7–B											
ct–	-2.1	0	-3.2	0.4	3	6.2				2204	R
mr_T1	-2.9	0.6	-3.7	0.1	2.7	6.1	0.993	1.005	0.993	2250	S
ct–	-4.1	3.8	-4.1	1.2	2.4	5.5				1692	R
mr_T2	-1.9	6.2	-3	-1	3.5	6.2	1.019	1.008	1.004	2059	S
mr_MP–	0	4	-5	0	0	0				2266	R
mr_T2	1.9	4.3	-4.9	0	0	-0.1	1.019	1.001	1	2403	S
Patient 8–B											
ct–	0.3	12.2	6.8	-18.6	-6.2	-4.9				1258	R
mr_T1	-2.6	9.1	11.8	-17.8	-1.4	-6.6	0.967	0.964	1.045	1586	S
ct–	1.2	13.6	-1.3	-11.1	-4.6	-6.6				2154	R
mr_T2	1.8	12.3	-0.2	-10.9	-4.6	-6.8	1.007	0.99	1.006	2222	S
mr_MP–	1.3	3	-3.6	0.8	1.9	0.7				1955	R
mr_T2	3.6	1.8	-1.7	0.3	0.8	0	1.025	0.988	1.009	2120	S
Patient 9–B											
ct–	-5.4	3.7	0.6	-5.8	-4.7	0.6				2055	R
mr_T1	-5.6	0.5	-2.2	-3.5	-4.4	1.8	0.99	0.984	0.98	2442	S
ct–	-5.3	5.6	-17	-4	-4.1	1.9				2363	R
mr_T2	-4.1	5.5	-15.5	-4.6	-3.4	1.5	1.012	0.995	1.011	2561	S
mr_MP–	1	2	-4	0	0	0				2484	R
mr_T2	3.5	2.3	-3.8	-0.1	0	-0.3	1.024	0.998	1	2817	S

Modality	Translation		
	x	y	z
Patient 1–A			
ct	8.34003	0.262589	0
mr_PD	7.3463	24.3232	4
mr_PDR	4.90396	20.0383	1
mr_T1	7.17767	19.869	4
mr_T1R	5.05547	20.1008	1
mr_T2	6.10577	22.7906	13
mr_T2R	3.13588	18.5162	2
Patient 2–A			
ct	4.39003	-0.370514	0
mr_PD	9.1636	15.6139	18
mr_PDR	6.92824	15.535	16
mr_T1	6.79765	7.42761	19
mr_T1R	4.80202	11.6861	17
mr_T2	7.01407	13.938	25
mr_T2R	4.75209	5.20282	48
Patient 3–A			
ct	2.68318	-13.9024	0
mr_PD	8.11717	18.0157	36
mr_PDR	6.85913	20.1418	36
mr_T1	4.69096	22.7863	35
mr_T1R	3.52538	22.6158	34
mr_T2	6.64104	17.8256	40
mr_T2R	5.64468	19.2543	40
Patient 4–A			
ct	5.65477	-0.796539	0
mr_PD	8.63837	19.3867	35
mr_PDR	7.39346	22.0534	34
mr_T1	5.89629	18.4892	34
mr_T1R	6.54546	23.05	32
mr_T2	7.85771	12.3336	37
mr_T2R	6.93391	21.4912	36
Patient 5–A			
ct	0.979782	-14.1332	0
mr_PD	7.82187	18.8854	19
mr_PDR	8.00098	21.0758	17
mr_T1	8.22556	21.0891	19
mr_T1R	8.64044	23.1814	17
mr_T2	8.39204	19.8978	36
mr_T2R	8.48778	20.9432	34
Patient 6–A			
ct	3.05191	-0.0773315	0
mr_PD	9.64647	24.0595	24
mr_PDR	7.09732	23.281	22
mr_T1	6.42091	21.7762	24
mr_T2	7.31889	24.2898	26
mr_T2R	5.00537	21.7055	24
Patient 7–A			
ct	1.97609	4.50055	0
mr_PD	8.10493	24.1277	8
mr_PDR	5.34363	18.4845	5
mr_T1	4.52769	23.428	8
mr_T1R	3.07294	24.1205	5
mr_T2	7.36554	22.4286	10
mr_T2R	4.94936	18.1313	8
Patient 1–B			
ct	9.8352	-3.01395	0
mr_PD	-1.42426	4.11234	2
mr_T1	0.358932	4.35963	5
mr_T2	-1.13695	-4.22468	0
mr_MP	23.6522	-5.34918	66
Patient 2–B			
ct	-5.21332	-7.19392	0
mr_PD	-5.0509	5.44126	3
mr_T1	-4.69702	6.51001	3
mr_T2	-4.0221	3.14245	2
mr_MP	22.9696	4.69599	48
Patient 3–B			
ct	5.72956	1.7956	0
mr_PD	9.15237	-0.89769	19
mr_T1	6.92894	6.51906	19
Patient 4–B			
ct	10.1349	-2.88666	0
mr_PD	5.09914	3.28878	4
mr_T1	3.49558	4.19601	2
mr_T2	1.87157	-0.455582	1
mr_MP	18.0773	15.0026	67
Patient 5–B			
ct	8.38589	-7.81199	0
mr_T1	-3.00654	0.835381	26
mr_T2	-2.34953	1.7034	24
mr_MP	-12.6107	7.82873	67

Modality	Translation		
	x	y	z
Patient 6–B			
ct	3.44701	0.145782	0
mr_T1	-0.00256348	-0.699112	18
mr_T2	0.377914	-3.45106	15
mr_MP	2.40002	0.437576	79
Patient 7–B			
ct	0.904816	0.621567	0
mr_T1	7.97235	2.18253	18
mr_T2	9.26294	-2.93028	17
mr_MP	8.63542	7.95525	77
Patient 8–B			
ct	2.47636	10.9551	0
mr_T1	-2.854	6.72024	26
mr_T2	-3.1254	1.78926	25
mr_MP	-5.66479	0.121559	62
Patient 9–B			
ct	3.23119	4.97693	0
mr_T1	-5.52097	-3.49944	22
mr_T2	-4.99231	-7.23582	6
mr_MP	-4.89862	8.62264	48

Appendix D

Interpolation grids

Following we describe the local deformation model applied to the retinographies (section 3.5, page 3.5). It can be found in many image processing references, for instance [69].

A set of control points defines an output-input mapping function M. This mapping must be applied to each coordinate in the image, which determines a high computational cost, specially for complex functions such as high degree polynomials. However, M is usually a smooth function, i.e. it has small derivative $\frac{\partial M}{\partial i}, \frac{\partial M}{\partial j}$ values. Therefore, it can be approximated in a local fashion by other simpler functions.

The explicit computation of M will be done only for the points belonging to a grid, while interpolating the others. Let t be the interpolation step, and

$$(k, l) = M(i, j) = (M_x(i, j), M_y(i, j))$$

the output-input mapping.

We are searching $M(i + u, j + v), 1 \leq u, v \leq t - 1$ integer, from the values $M(i, j), M(i+t, j), M(i, j+t), M(i+t, j+t)$. Then we need to interpolate (figureD.1):

$$M_x(i + u, j + v) \text{from} M_x(i, j), M_x(i + t, j), M_x(i, j + t), M_x(i + t, j + t)$$

and similarly

$$M_y(i + u, j + v) \text{from} M_y(i, j), M_y(i + t, j), M_y(i, j + t), M_y(i + t, j + t)$$

The simplest interpolation scheme is the linear, but since M_x and M_y are function of two variables, we would have to interpolate a plane from four points, which is an over-dimensioned problem. The function of two variables next in simplicity to the plane is called hyperbolic paraboloid:

$$f(x, y) = ax + by + cxy + d \tag{D.1}$$

and its interpolation is bilinear, because taking one variable as a constant value, the other one become linear. Let's say we want to interpolate the four points $f(x_0, y_0)$, $f(x_0, y_1)$, $f(x_1, y_0)$ and $f(x_1, y_1)$. The equations of coefficients a, b, c, d are deduced from the following algorithm, which finds the value of $f(x, y)$ for some point $x_0 < x < x_1, y_0 < y < y_1$ (figure D.2) :

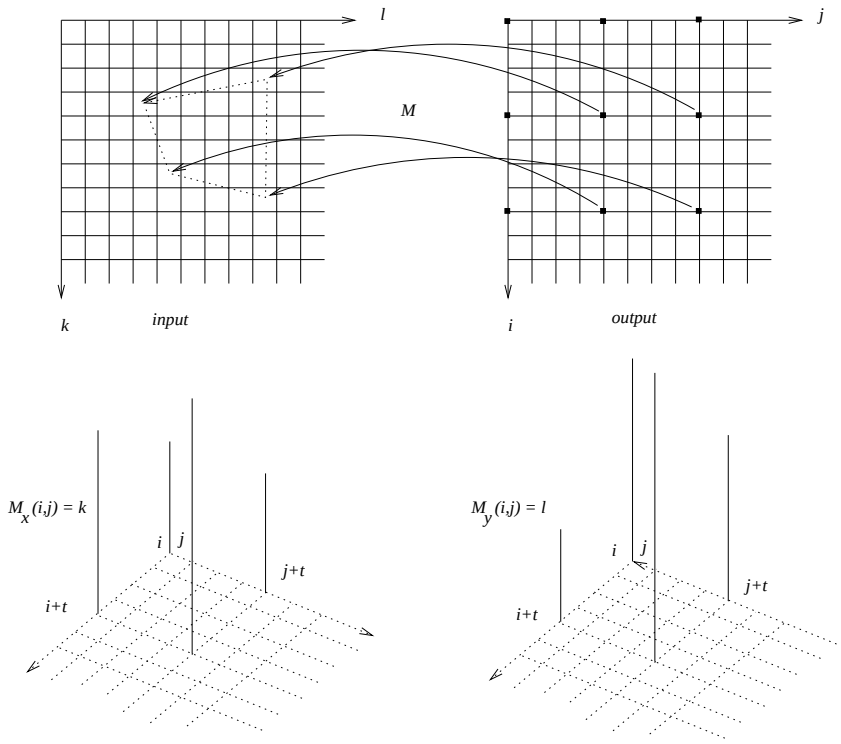

Figure D.1: Interpolation grid with step $t = 4$.

1. interpolate a straight line between $f(x_0, y_0)$ and $f(x_1, y_0)$, to obtain:

$$f(x, y_0) = f(x_0, y_0) + x\Big[\frac{f(x_1, y_0) - f(x_0, y_0)}{x_1 - x_0}\Big]$$

2. again the same step with $f(x_0, y_1)$ i $f(x_1, y_1)$ to compute:

$$f(x, y_1) = f(x_0, y_1) + x\Big[\frac{f(x_1, y_1) - f(x_0, y_1)}{x_1 - x_0}\Big]$$

3. interpolate a straight line between $f(x, y_0)$ and $f(x, y_1)$ to find

$$f(x, y) = f(x, y_0) + y\Big[\frac{f(x, y_1) - f(x, y_0)}{y_1 - y_0}\Big]$$

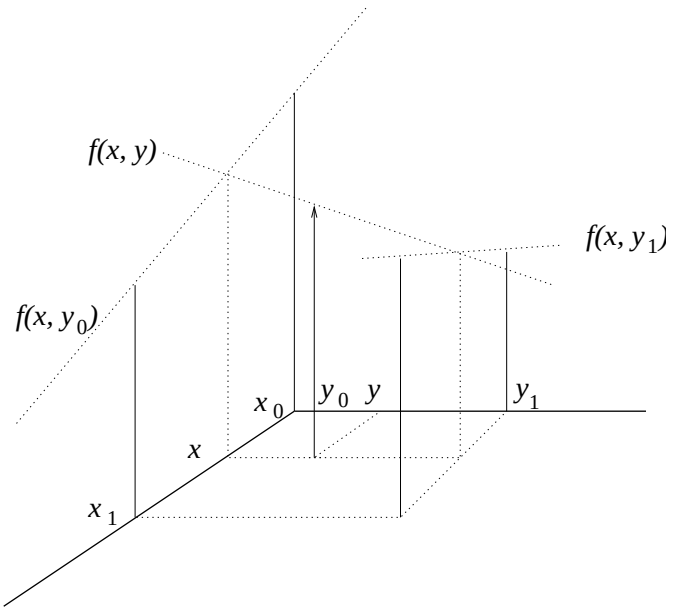

Figure D.2: Bilinear interpolation

From the previous, we deduce:

$$\begin{aligned} a &= \frac{f(x_1, y_0) - f(x_0, y_0)}{x_1 - x_0} \\ b &= \frac{f(x_0, y_1) - f(x_0, y_0)}{y_1 - y_0} \\ c &= \frac{f(x_1, y_1) + f(x_0, y_0) - f(x_0, y_1) - f(x_1, y_0)}{(x_1 - x_0)(y_1 - y_0)} \\ d &= f(x_0, y_0) \end{aligned} \tag{D.2}$$

A grid with enough density makes the mapping less computationally expensive, while losing little accuracy. The grid space depends on the transformation model; for Landsat MSS, it is 80 pixels wide.

Appendix E

A model of the eye

In this appendix, we will give a numerical model of the acquisition of fundus images by a camera. We will consider the model shown in figure E.1; a represents the image seen in flat coordinates at the camera, and S the deformed coordinates at the fundus. We are interested in the geometric correspondence between the two coordinate systems.

E.1 Translating from camera to fundus coordinates.

Given a, the problem is to find S. Let's consider a system coordinates with origin in the centre of the circle. We build a line passing through the point a and the pinhole centre. Their coordinates are $(-a, -G-F)$ and $(0, -G)$. The equation of the line is:

$$\begin{cases} x = & a\lambda \\ y = & F\lambda - G \end{cases} \tag{E.1}$$

Let's find the intersection between the line and the circle, (x_c, y_c):

$$x_c^2 + y_c^2 = R^2 \tag{E.2}$$

Squaring with E.1, we obtain an equation of λ:

$$\lambda^2(F^2 + a^2) - 2FG\lambda + G^2 - R^2 = 0 \tag{E.3}$$

which solves to

$$\lambda_{1,2} = \frac{FG \pm \sqrt{F^2R^2 + a^2R^2 - a^2G^2}}{F^2 + a^2} \tag{E.4}$$

Choosing λ_1 because it is the largest, corresponding to the furthest of the two points,

$$\begin{cases} x_c = & a\lambda_1 \\ y_c = & F\lambda_1 - G \end{cases} \tag{E.5}$$

Then

$$\alpha = \arctan \frac{x_c}{y_c} \tag{E.6}$$

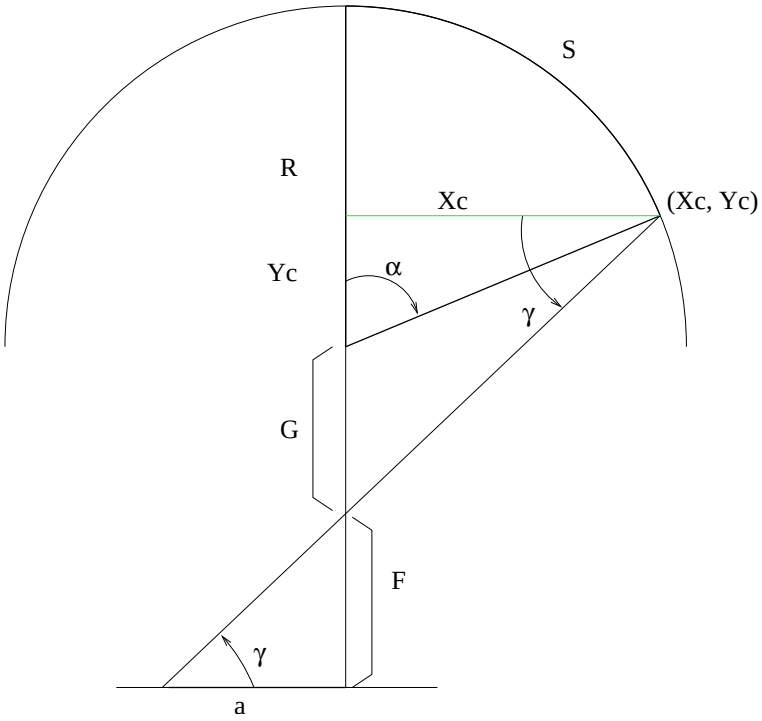

Figure E.1: Geometric model of the eye

And finally

$$s = \alpha R \tag{E.7}$$

E.2 Translating from fundus to camera coordinates

The problem is: given S, find a. The coordinates of (x_c, y_c) are:

$$\alpha = \frac{S}{R} \tag{E.8}$$

$$(x_c, y_c) = (R\sin\alpha, R\cos\alpha) \tag{E.9}$$

The line passing through this point and the pinhole centre is:

$$\begin{cases} x = & x_c\lambda \\ y = & (y_c + G)\lambda - G \end{cases} \tag{E.10}$$

And its intersection to the line at the bottom, $y = -G - F$,

$$a = -x_c \frac{F}{y_c + G} \tag{E.11}$$

E.3 Preliminary results

We have not implemented the optimisation scheme proposed in chapter 3. However, it is interesting to note that the global deformation achieved with this model (figure E.2) is visually very similar to that we want to model (top). Results so far suggest this scheme is worth a full development.

1. Translate all the transformation parameters from the standard flat model to the fundus coordinates.
2. Iterate global geometric parameters until a maximum is achieved.
3. Iterate the registration for each frame until a maximum is achieved
4. Repeat step 2) until successful convergence.

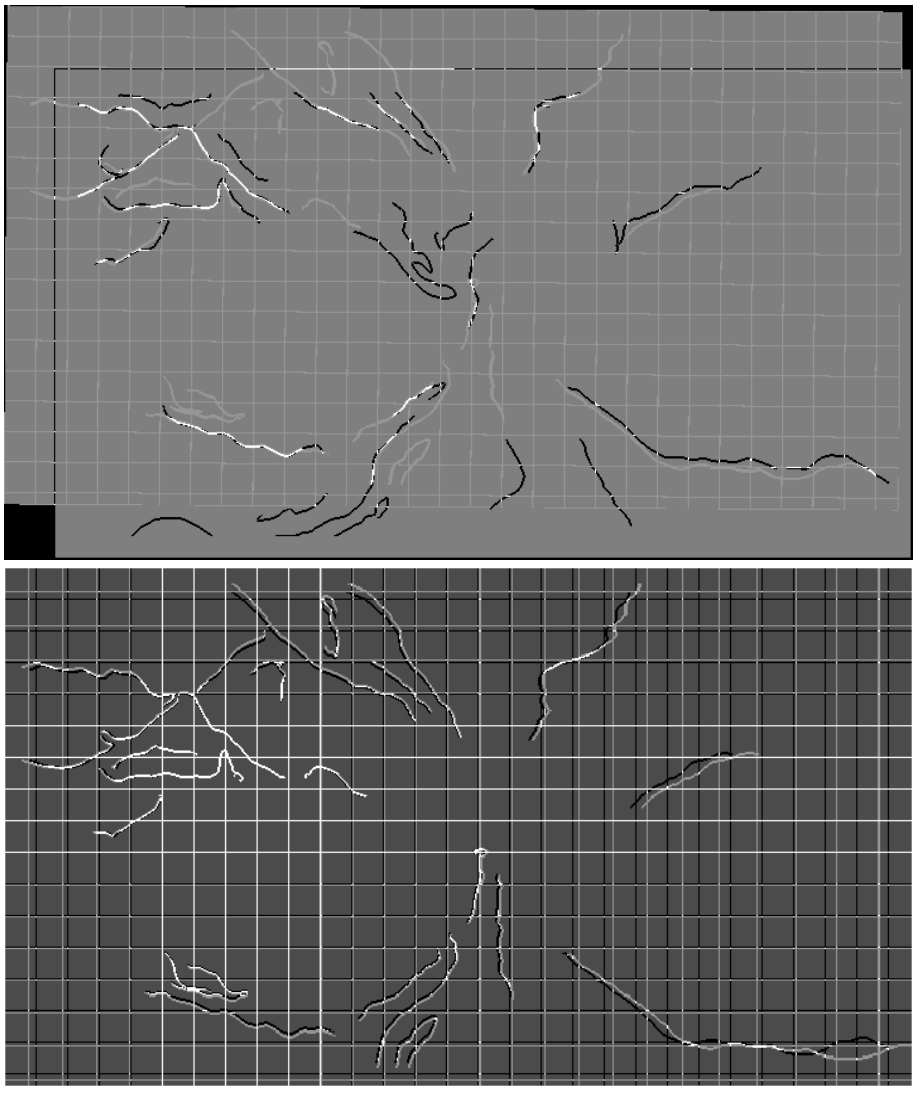

Figure E.2: Top: typical local misregistration. Bottom: deformation achieved using the model described.

Appendix F

Registration results for pairs of 2D images

Although in chapter 3 we have worked only with ophthalmologic medical images, results are valid for any 2-D images showing creaseness-like features. For instance, in satellite images the roads and coast like would serve this purpose.

We have tried our algorithm for two pairs of pictures from Michelangelo's Pietà IBM project [34], gently provided by Dr. Frederic Leymarie. We have run the method without any modification, using as landmarks the marks of the hammer. Check the correctness of matching at the overlapping areas.

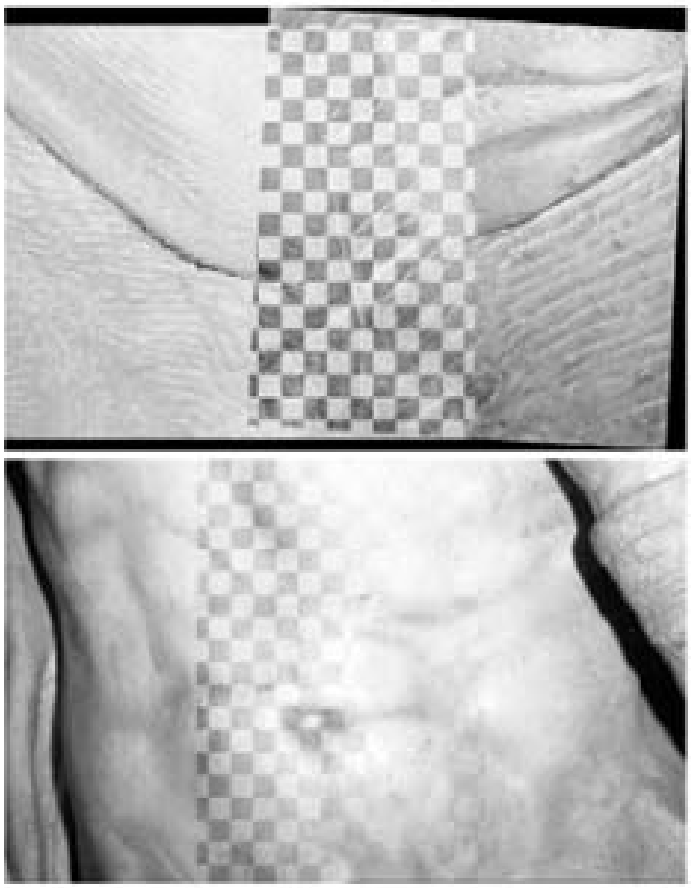

Figure F.1: Registration applied to two partially overlapping images of a statue. The marks of the hammer have been extracted with also with creases, and the standard registration algorithm has aligned them. The presentation here shows mosaicing at the common regions.

Appendix G

Levenberg-Marquardt optimisation

The purpose of this appendix is to explain the numerical methods employed in chapter 4, mainly the Levenberg-Marquardt method to estimate parameters of a non-linear model. Although brief, the explanation should be useful to clarify the terminology appearing in that chapter, and also to provide some basis for their final conclusions. To write this appendix I have followed the indication of Sadler's short but excellent book [89] and the corresponding Numerical Recipes' chapter [80], while final improvement have been taken from Cambridge's papers [79].

G.1 Introduction to model-based maximisation

The problem to be solved here appears in the context of estimation of model parameters. The situation is as follows: in an experiment we are able to predict some measurable value by means of some function of parameters of the experiment. The function expresses to our knowledge the relationship between the parameters and the output value. We may be able to measure some of the parameters, and also we must be able to measure the actual output value, and our aim is to estimate the remaining set, unknown, parameters.

Written in a mathematical expression,

$$Y = f(\mathbf{x}; \mathbf{a}) + \epsilon \tag{G.1}$$

where $\mathbf{x}$ is the vector of $\mathbf{M}$ parameters to be estimated
$\mathbf{a}$ represents a vector of some measured variables
ϵ is the unknown random error
Y represents the dependent variable
f the population regression function (PRF), given the functional relationship between Y, $\mathbf{x}$ and $\mathbf{a}$

For the experiment of the ultrasound calibration,

- $\mathbf{a}$, the known parameters, are the coordinates of the object in the ecography (u_x, u_y), and the receiver to transmitter matrix, M_R^T .
  $\mathbf{a} = \{(u_x, u_y), M_R^T\}$

- The parameters to be estimated, $\mathbf{x}$, are: the ultrasound-to-receiver matrix, M_U^R , and, as a by-product, M_T^C .
  $\mathbf{x} = \{M_U^R\ , M_T^C\ \}$
- $\mathbf{f}$ provides the position in the cuberille of any pixel coordinates (u_x, u_y).

For the sake of comprehension, we recall equation 4.1:

$$(x', y', z') = f(\mathbf{x}; \mathbf{a}) = (u_x, u_y, 0, 1) \cdot M_U^R\ (\mathbf{x}) \cdot M_R^T\ \cdot M_T^C\ (\mathbf{x})$$

Suppose that a total of $\mathbf{N}$ replicates of the experiment have been made. For each observation, let y_i denote the observed value, Y_i the predicted value, and similarly $\mathbf{a}_i$ and $\mathbf{x}_i$ the measured and estimated parameters. The ith residual is defined as the difference between the actual and expected values:

$$e_i = y_i - Y_i \tag{G.2}$$

And the objective function $\mathbf{S}(\mathbf{x})$ to be minimised:

$$\mathbf{S}(\mathbf{x}) = \sum_{i=1}^{N} e_i^2 = \sum_{i=1}^{N} \{y_i - f(\mathbf{x}; \mathbf{a}_i)\}^2 \tag{G.3}$$

For $\mathbf{S}$ being a linear function of $\mathbf{x}$, minimising $\mathbf{S}$ is known as linear least squares. Here we will focus on non-linear least squares, since the matrices required for the calibration include sinusoidal functions.

G.2 Complementary terms

Before proceeding on, we will develop the terms that will be useful to define some maximisation strategies.

The gradient of $\mathbf{S}$, or Jacobian, point toward the direction of maximum increase. It is a vector of $\mathbf{M}$ components, one for each independent variable:

$$\mathbf{J} = \nabla \mathbf{S} = \left[\frac{\partial \mathbf{S}(\mathbf{x})}{\partial x_1}, \ldots, \frac{\partial \mathbf{S}(\mathbf{x})}{\partial x_{\mathbf{M}}} \right]_{\mathbf{x}=\mathbf{x}_j}^T \tag{G.4}$$

Each term can be developed; note the final expression demands explicit calculation of ∂f

$$\frac{\partial \mathbf{S}(\mathbf{x})}{\partial x_j} = 2 \sum_{i=1}^{N} e_i \frac{\partial e_i}{\partial x_j} = -2 \sum_{i=1}^{N} e_i \frac{\partial f(\mathbf{x}; \mathbf{a}_i)}{\partial x_j} \tag{G.5}$$

The Hessian of $\mathbf{S}$ is a $\mathbf{M} \times \mathbf{M}$ matrix where each term is a second-order derivative of $\mathbf{S}$. A usual approximation, the Gaussian, requires only first-order derivatives:

$$\mathbf{H} \simeq \mathbf{G} = 2 \sum_{i=1}^{N} \nabla f_i \nabla f_i^T \tag{G.6}$$

where the gradient of f is:

$$\nabla f_i = \left[\frac{\partial f(\mathbf{x}; \mathbf{a}_i)}{\partial x_1}, \ldots, \frac{\partial f(\mathbf{x}; \mathbf{a}_i)}{\partial x_{\mathbf{M}}} \right]^T_{\mathbf{x}=\mathbf{x}_j} \tag{G.7}$$

A related measure is the so-called curvature matrix α,

$$\alpha = \frac{\mathbf{H}}{2} \tag{G.8}$$

G.3 Maximisation techniques

Now, we briefly define two search methods, steepest descent and parabolic approximation, and see how both can be combined into a single and more powerful combination, the Levenberg-Marquadt method.

Maximisation algorithms seek an iteration of estimating values $\mathbf{x}_j$ to decrease the value of the objective function $\mathbf{S}$:

$$\mathbf{S}(\mathbf{x}_{j+1}) < \mathbf{S}(\mathbf{x}_j) \tag{G.9}$$

A plethora of maximisation methods exists; for our purpose, we choose those that:

- make use of the explicit the derivative of $\mathbf{S}$
- the function can be tested for a number of replicates of an experiment.

The ultrasound calibration requirements are somewhat special in the sense that we suppose Y_i to be constant and nil; in our model, $f(\mathbf{x}; \mathbf{a}) = (x', y', z')$ will be set to:

- **Bottom of the recipient** we set the line appearing in the image to be the bottom place of the cuberille, thus the requirement $z' = 0$ will give one equation to be minimised, $f_x = 0$
- **Single point** will lead to $x' = y' = z' = 0$. We must combine the three resulting equations into a single one, $f_x^2 + f_y^2 + f_z^2 = 0$.
- **Line** will lead to $x' = y' = 0$, which, put into a single equation, is: $f_x^2 + f_y^2 = 0$.

Calibration is also at the heart of experimental and autonomous robotics; in robots, each joint axis needs to be calibrated. It is interesting to review related problems in papers from this area, specially Hollerbach and other 's [32, 33, 35]. For instance, his classification of calibration methods as:

- Open-loop methods, which employ an external metrology to estimate the actual value y_i, this is, the actual position of the end-loop (for robots) or the calibrating object (for ecographies)
- Closed-loop methods constraint the movements, for instance to the ground, so y_i is set to zero for all cases. Constraints may be of one degree (plane) to three degrees (point)

Our calibration methods are included in the close-loop category.

G.3.1 Steepest descent

The steepest descent method exploits the property of the negative gradient to point at a given point toward the maximum decreasing direction.

$$\mathbf{x}_{j+1} = \mathbf{x}_j - h\ I\ \mathbf{J} \tag{G.10}$$

where $\mathbf{x}_j$ is current estimation of parameters
$\mathbf{x}_{j+1}$ is the new estimation to be evaluated
$\mathbf{J}$ is the gradient of $\mathbf{S}$, or Jacobian, pointing toward the steepest ascend.
h determines the length of the step
I is the $\mathbf{M} \times \mathbf{M}$ unity matrix, included to simplify later discussion

Figure G.1 shows graphically that direction chosen at a point is along the gradient. Although any value of h could be taken, normally a linear search is performed along the line until the lowest value is reached.

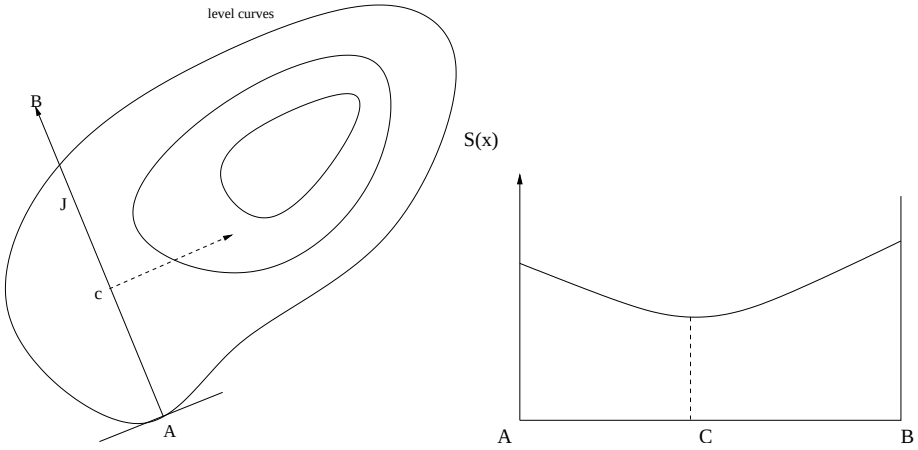

Figure G.1: *A* labels the point $\mathbf{x}_j$, *B* labels $\mathbf{x}_{j+1}$ The steepest descent maximisation follows the opposite direction of the gradient or Jacobian J (left). The length of the step may be taken to the minimum value along the line (right).

G.3.2 Parabolic or Newton maximisation

Another techniques consists of approximating $\mathbf{S}$ locally by some other more tractable function with an analytical minimum. For the one-dimensional case, shown in figure G.2, the function is approximated by a parabola. The minimum of the approximated parabola is chosen as the next estimated step.

In $\mathbf{M}$ dimensions, the iterative formula which reflects this idea is:

$$\begin{aligned} \mathbf{x}_{j+1} &= \mathbf{x}_j - \mathbf{H}^{-1}\mathbf{J} \\ &\simeq \mathbf{x}_j - \mathbf{G}^{-1}\mathbf{J} \end{aligned} \tag{G.11}$$

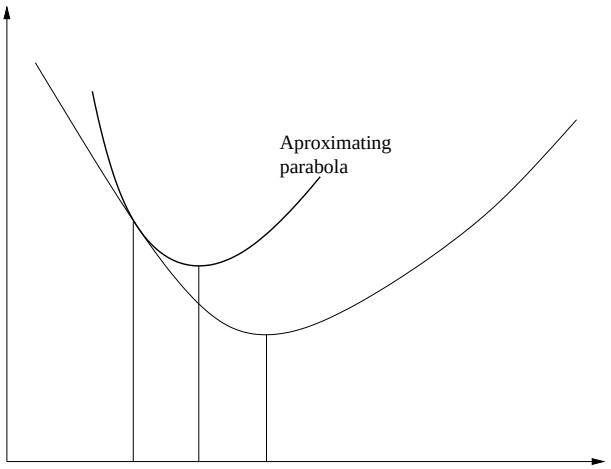

Figure G.2: The parabolic approximation to **S** permits to compute the new step x_2 where a minimum is expected.

G.3.3 Levenberg-Marquardt

The two methods above can be seen as complementary; steepest descent works robustly, although it has low rate of convergence. Newton method has second-order convergence property near the minimum, but has poor performance otherwise.

Equations G.10 and G.11 are combined into a single one:

$$\mathbf{x}_{j+1} = \mathbf{x}_j - (\mathbf{G} + h\mathbf{I})^{-1}\mathbf{J} \tag{G.12}$$

which is usually written equivalently as:

$$(\mathbf{G} + \mu\mathbf{I})\,\Delta\mathbf{x} = -\mathbf{J} \tag{G.13}$$

where $\Delta\mathbf{x} = \mathbf{x}_{j+1} - \mathbf{x}_j$ is the correction vector

μ is a positive constant evaluated at every iteration. As convergence is successful, μ decreases, otherwise it increases.

Equation G.13 is numerically easier to solve than G.12, because does not need explicit calculation of the inverse matrix and can use that symmetry properties of $(\mathbf{G} + \mu\mathbf{I})$.

We will not write here the details of the algorithm, such as the adjustment of the combining parameter μ or the stopping conditions. Simply remarks that:

- for $\mu \to 0$, the method becomes Newton's.
- for $\mu \to \infty$, then $\mathbf{G}$ in the sum $(\mathbf{G} + \mu\mathbf{I})$ becomes a minor perturbation, and the method resembles steepest descent.

Figure G.3 shows graphically that the correction vector is a parametric combination of the two methods.

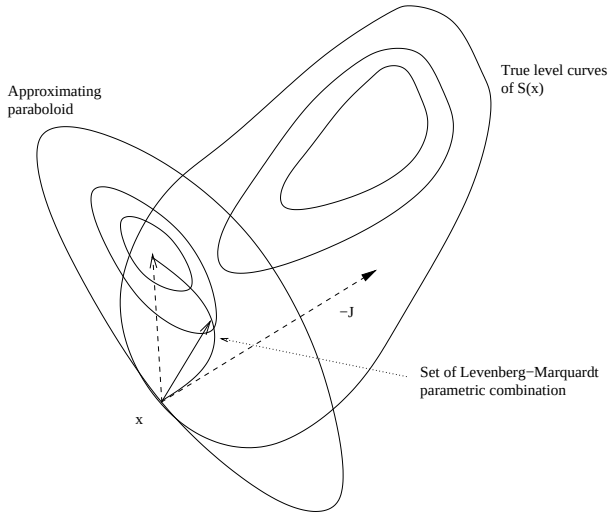

Figure G.3: Steepest descend and Newton method may be balanced to achieve the best of both.

G.4 Further requirements

The optimisation algorithm convergence to a parameter set $\mathbf{x}^*$ may not necessarily imply the correctness of the solution or, even worse, the suitability of our model to the experiment. The covariance of the standard errors in the fitter parameters $\mathbf{x}$ can be estimated evaluating the Hessian:

$$C \equiv \alpha^{-1} = \left(\frac{\mathbf{H}}{2}\right)^{-1} \tag{G.14}$$

Other measures were first proposed i the field of robot-kinematic calibration; well-posed problems are identified by rank determination and scaling.

We perform singular value decomposition of the Jacobian matrix at $\mathbf{x}^*$:

$$\mathbf{J} = \mathbf{U}\Sigma\mathbf{V}^T \tag{G.15}$$

where $\Sigma = \mathrm{diag}(\mu_1, \ldots, \mu_{\mathbf{M}})$ is the list of ordered decreasing singular values of $\mathbf{J}$. Any μ too near to zero will imply a non-identifiable parameter. Otherwise, the matrix has full rank, and the so-called condition number (C.N.)

$$k = \frac{\mu_1}{\mu_{\mathbf{M}}} \tag{G.16}$$

A large condition number (higher than 100) indicates that the problem is ill-posed. You may refer to [39], page 50 for strict mathematical description, or [79] for a plainer explanation.

The other issue is parameter scaling: the optimisation models described above do not take into account that parameters have different units and also different range of

values, which make the search space liable to have an elliptical shape. **S** may be very sensitive to variations of one parameter, while the same variations in another produce no effect. The model then becomes ill-posed. You may refer to [39], page 185 for strict mathematical descriptions.

The best way to solve this problem is by parameter scaling. In equation G.13, instead of **J** we use **JH**, where $\mathbf{H} = \mathrm{diag}(h_1, \ldots, h_q)$ is a diagonal matrix such that:

$$h_i = \begin{cases} \|j_i\|^{-1} & : \quad \|j_i\| \neq 0 \\ 1 & : \quad \|j_i\| = 0 \end{cases} \tag{G.17}$$

where j_i is the ith column of **J** evaluated near the solution (thus without scaling).

Finally, the solution $\mathbf{x}'$ of the system with this settings will have to be re-scaled to obtain the true parameters **x**:

$$\mathbf{x}' = \mathbf{H}^{-1}\mathbf{x} \tag{G.18}$$